energies

MDPI

Review

Looking for an Optimal Composition of Nickel-Based Catalysts for CO_2 Methanation

Guido Busca [1,2,*], Elena Spennati [1,2], Paola Riani [2,3] and Gabriella Garbarino [1,2,4]

1 Dipartimento di Ingegneria Civile, Chimica e Ambientale, Università di Genova, Via Opera Pia 15, 16145 Genova, Italy; elena.spennati@edu.unige.it (E.S.); gabriella.garbarino@unige.it (G.G.)
2 Consorzio Interuniversitario Nazionale di Scienza e Tecnologia dei Materiali (INSTM), UdR di Genova, Via Dodecaneso 31, 16146 Genova, Italy; paola.riani@unige.it
3 Dipartimento di Chimica e Chimica Industriale, Università di Genova, Via Dodecaneso 31, 16146 Genova, Italy
4 CNR-SCITEC G. Natta, Via Golgi 19, 20133 Milano, Italy
* Correspondence: guido.busca@unige.it; Tel.: +39-010-335-6024

Abstract: AbstractA detailed critical analysis of the scientific literature data concerning catalysts for CO_2 methanation based on nickel supported over oxides was performed. According to the obtained information, it seems that an ionic support is necessary to allow a good nickel dispersion to produce very small nickel metal particles. Such small metal particles result in being very active toward methanation, limiting the production of carbonaceous materials. The use of support and/or surface additives gives rise to medium surface basicity, allowing medium-strong adsorption of CO_2, and it is also advisable to increase the reaction rate. A medium nickel loading would allow the free support geometric surface to be covered densely by small nickel metal particles without the production of larger Ni crystals. It is also advisable to work at temperatures where $Ni(CO)_4$ formation is not possible (e.g., >573 K). The promising properties of systems based on doped Ni/Al_2O_3, doped with basic and re-active oxides such as MnO_x or/and CeO_2, and those based on Ni/CeO_2 were underlined.

Keywords: CO_2 hydrogenation; methanation; reverse water gas shift; substitute natural gas; nickel catalysts; carrier; support; carbon residues; deactivation; promoters

Citation: Busca, G.; Spennati, E.; Riani, P.; Garbarino, G. Looking for an Optimal Composition of Nickel-Based Catalysts for CO_2 Methanation. *Energies* **2023**, *16*, 5304. https://doi.org/10.3390/en16145304

Academic Editor: Giorgio Vilardi

Received: 1 June 2023
Revised: 3 July 2023
Accepted: 5 July 2023
Published: 11 July 2023

1. Introduction

The methanation of captured CO_2 using green hydrogen is considered a possible way to valorize and reuse it, also in view of the so-called "power to Gas" technologies [1,2]. The new process to be designed for CO_2 methanation [3] is strictly related to ones developed decades ago for Substitute Natural Gas (SNG) production from CO-rich syngases [4]. It possibly implies a CO_2 purification step followed by a catalytic reaction step. Depending on the performances and design of the catalytic reactor and on the final use of the produced methane, the following steps may be needed: condensation and removal of coproduced water, product separation from unreacted CO_2 and/or hydrogen (that can be recycled to the reactor), and separation from byproducts, such as CO and/or other hydrocarbons or oxygenated compounds. Thus, as always for industrial chemical plants, the key step for an efficient process is to develop high activity and high selectivity catalysts, just to reduce the onerousness of the separation and recycling steps and to maximize productivity. Although artificial intelligence-based methods are under development for discovering new and better catalysts for industrial chemical reactions [5], up to now, empirical methods based on human intelligence still represent the most reliable approach, in our opinion.

2. Thermodynamics of CO_2 Hydrogenation

The CO_2 methanation reaction,

$$CO_2 + 4\,H_2 \leftrightarrows CH_4 + 2\,H_2O$$

also denoted as the "Sabatier reaction", is an exothermic equilibrium reaction: thus, it is most favored at low temperatures and high pressures. However, according to its large exothermicity (ΔH°_{298} = −165 kJ/mol), the theoretical thermodynamic methane yield approaches totality at temperatures up to 473 K, also at 1 atm [6,7]. At higher temperatures, CO_2 conversions and methane yields allowed by thermodynamics decrease. However, methane synthesis is competitive with the production of CO through the so-called "reverse Water Gas Shift" reaction, rWGS,

$$CO_2 + H_2 \leftrightarrows CO + H_2O$$

which is weakly endothermic (ΔH°_{298} = +41.16 kJ/mol) and almost independent from reaction pressure; thus, its equilibrium is shifted to products the higher the temperature is. Thus, thermodynamically allowed CO_2 conversion will increase again, and at higher temperatures, CO will become the predominant product [6]. However, given the strong dependence of methanation on, and the almost independence of rWGS from, total pressure, at higher pressures the temperature range where methanation is predominant will increase to higher temperatures. In Figure 1, the resulting CO_2 conversions and CH_4 and CO yields at thermodynamic equilibrium are reported, as a function of temperature, at 0.1, 2.03, and 20.3 MPa.

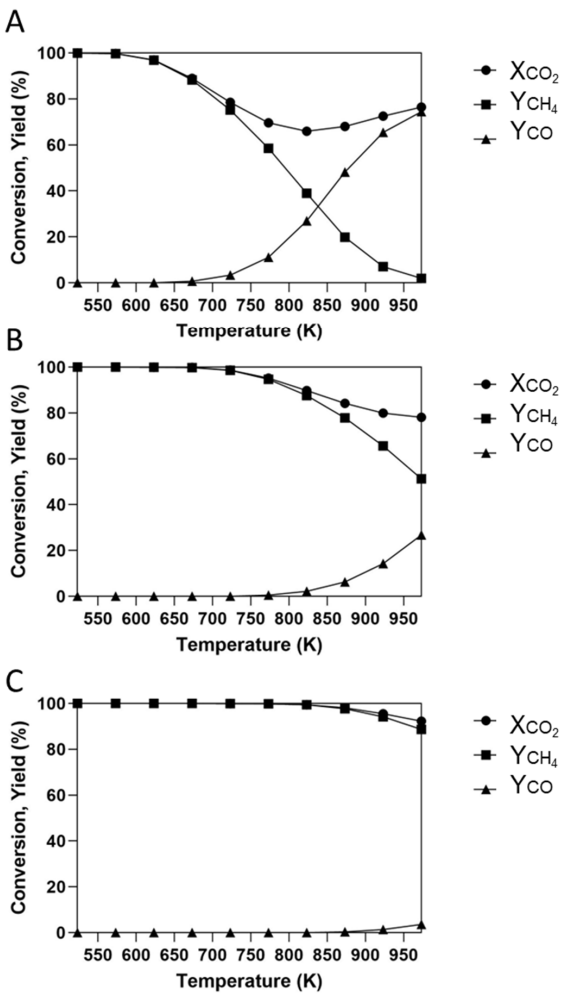

Figure 1. Equilibrium CO_2 conversion and CH_4 and CO yields (**A**): at 0.1 MPa; (**B**): at 2.03 MPa; and (**C**): at 20.3 MPa. Starting molar ratio H_2/CO_2 = 5. Calculated using a Gibbs reactor and Soave–Redlich–Kwong equation of state [8] and allowing a calculated phase for the reaction.

The production of higher hydrocarbons (paraffins and olefins), as it occurs in the so-called CO_2-Fischer Tropsch process, through the following reactions,

$$n\ CO_2 + (3n + 1)\ H_2 = C_nH_{2n+2} + 2n\ H_2O \qquad n > 1$$

$$m\ CO_2 + 3m\ H_2 = C_mH_{2m} + 2m\ H_2O \qquad m > 1$$

also represent competitive reactions, in principle. These reactions, which are also exothermic equilibrium reactions most favored at low temperature and high pressure, are less favored than methanation and may be realized in conditions where rWGS is still not favored. The higher hydrocarbon yield, forecasted at thermodynamic equilibrium at atmospheric pressure, is extremely low, and methane also remains the most favored hydrocarbon product at higher pressures [9].

According to Gao et al. [6] and our own thermodynamic calculations, carbon formation theoretically does not occur when the starting molar ratio is $H_2/CO_2 = 4$, while it should occur at $T < 873$ K when $H_2/CO_2 = 2$. In contrast, the calculations of Schmider et al. [10] report the formation of significant amounts of carbon by CO_2 hydrogenation with $H_2/CO_2 = 4$ at atmospheric pressure, with a maximum amount at around 800 K, which almost disappears if reaction pressure is raised to 2 MPa.

Thus, the overall available thermodynamic data indicate that, in principle, the best conditions for an industrial CO_2 methanation process are to realize the reaction in the presence of a selective catalyst for methanation, with low or no activity for reverse water gas shift and higher hydrocarbon synthesis, with a moderate H_2 excess ($H_2/CO_2 > 4$) working at $T < 650$ K or less at a moderately high pressure (1–2 MPa) to push conversion and selectivity to methane, limiting coproduction of CO and carbon deposition. In addition, the adoption of high space velocities will limit the significant production of higher hydrocarbons, achieving high CH_4 productivity.

To test and develop optimal catalysts, however, conditions in which possible limits become evident may give more information. To evidence and compare intrinsic catalytic activity and selectivity toward methane, as well as stability with respect to carbon deposition phenomena, studies realized at atmospheric pressure are more informative than those realized at high pressures [11], where the production of CO and carbon are essentially thermodynamically not possible.

3. Nickel Catalysts for CO_2 Hydrogenation Reactions

As is well known, transition metals are the most catalytically active materials for hydrogenation reactions, at least in sulfur-free environments [12]. As mentioned above, CO_2 hydrogenation can produce CO by reverse water gas shift, methane, and any other hydrocarbon and oxygenated organic compound. According to the literature, while Cu- and Pd-based catalysts are very active for methanol and higher alcohol synthesis, and Fe, Co, and Ru catalysts are active for higher hydrocarbon synthesis, Ni and Ru are the most active for CO_x methanation reactions. In fact, commercial catalysts are available for methanation in CO-rich syngases [12]: they are essentially based on Ru/Al_2O_3 for low-temperature applications, mainly for the methanation of CO_x residues in hydrogen and ammonia synthesis gas. Ni/Al_2O_3 is used for the same application and for high-temperature applications for the production of SNG [13].

An enormous amount of research work was recently carried out concerning catalysts for CO_2 methanation. Several reviews collect such studies [14–17]. Most of these papers, however, when concerning catalyst composition, appear to be mere collections of data with poor criticism. According to the literature, the commercial catalysts for CO-rich syngas methanation are also active for pure CO_2 methanation, although the optimal composition for these quite different applications can be remarkably different. In fact, although CO methanation and CO_2 methanation are certainly related reactions, the two reactants CO and CO_2 have very different chemical and adsorption properties. CO adsorbs strongly, also at very low temperatures, on metal surfaces, including nickel [18], with which it can

even react in mild conditions, producing the volatile carbonyl compound $Ni(CO)_4$ [19]. Instead, the interaction of CO with oxides, such as catalyst carriers, is essentially weak [20]. In contrast, CO_2 interaction with metal surfaces may be relatively weak [21] and may dissociatively occur at moderate temperatures, such as on Ni [22]. Instead, CO_2 adsorption on metal oxides occurs at room and even lower temperatures and may be very strong with basic oxides, producing a number of surface and subsurface species [23,24] and sometimes bulk carbonates [21]. The stronger reactivity of CO_2 with oxide carriers suggests that the carrier can have a more relevant role in the kinetics of CO_2 hydrogenation than of CO hydrogenation.

Taking into account that nickel is by far cheaper than ruthenium and other noble metals, and that the reaction temperature for CO_2 methanation may not necessarily be so low, a large part of the current research is centered on nickel catalysts [25,26]. The main approach is to increase the low-temperature activity of Ni-based catalysts to retain total selectivity to methane, limiting deactivation phenomena.

3.1. Unsupported Nickel Catalysts

Unsupported Ni (nano)particles can be produced in several ways, as summarized by Abboud et al. [27]. The preparation of ferromagnetic Ni particles [28] can help in the recovery of the catalyst by magnetic methods or by using induction heating systems. Thermal stability against sintering is a main point concerning unsupported metal particles. Lucchini et al. [29] reported relevant sintering and consequent deactivation of differently prepared unsupported nickel nanoparticles upon CO catalytic hydrogenation experiments in the 550–800 K range.

CO_2 methanation was investigated on unsupported Ni metal particles produced by the reduction of NiO with H_2 by Garbarino et al. [30], Pandey et al. [31], Varvoutis et al. [32], and Kristiani and Takeishi [33], while Lee et al. tested Raney nickel [34]. Ni particles sized at 100–200 nm show moderate catalytic activity, definitely lower than for supported nickel [30,32]. Low Turn Over Frequency [33] but also low selectivities to methane with both coproduction of CO and a quite quick deactivation was associated with the production of encapsulating carbon and carbon nanotubes [30]; see Figure 2.

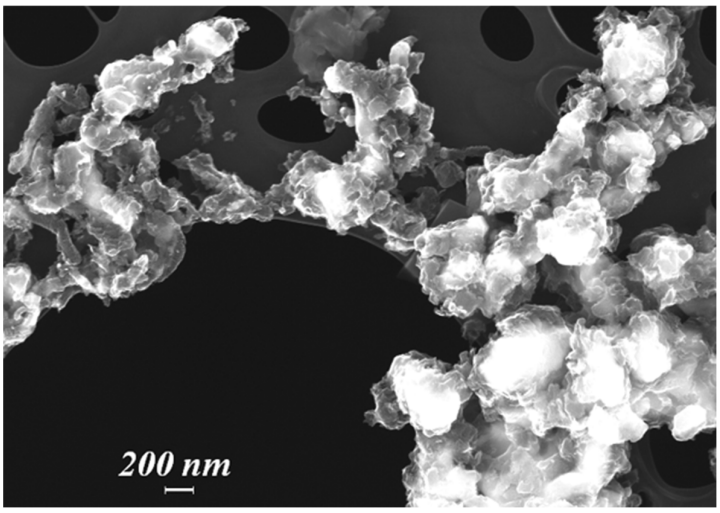

Figure 2. FE-SEM micrograph of spent unsupported Ni catalyst after methanation experiments showing Ni particles embedded in carbon residues. Modified from ref. [30].

Similarly, Hao et al. [35] reported low activity and low selectivity to methane over "bare nickel". According to Pandey [31], the moderate activity of pure nickel is significantly increased by the addition of small amounts of iron. On Raney nickel, selectivity to methane is reported to be not far from 100% for the purest Ni sample, which is also the most active [34]. Very small (d < 8 nm) unsupported nickel nanoparticles produced by the

reduction of $NiCl_2$*$6H_2O$ with $NaBH_4$ were found almost inactive in CO_2 methanation by Riani et al. [36]. However, it must be taken into account that such a preparation method may leave B impurities on the metal samples [37], which can affect catalytic behavior. Lan et al. [38] reported that the increase in the (111) to (200) crystal planes, obtained by exposing the catalyst to a magnetic field during preparation, enormously increases the catalytic activity of unsupported nickel at 453 K, with total methane selectivity.

3.2. Nickel Supported on Simple Metal Oxide Carriers

Several papers report a comparison of the catalytic activity of nickel catalysts supported on different simple oxide carriers for CO_2 methanation, with partially agreeing data. According to Muroyama et al. [39], the CO_2 conversion for most catalysts drastically increases at 498–523 K and reaches a maximal value at 573–623 K, approaching thermodynamically allowed values for the given conditions. The order of CH_4 yield at 523 K was as follows: Ni/Y_2O_3 > Ni/Sm_2O_3 > Ni/ZrO_2 > Ni/CeO_2 > Ni/Al_2O_3 > Ni/La_2O_3. The catalytic activity can be partly explained by the basic property of the catalysts. However, the same authors reported different scales for selectivity, with Ni/Al_2O_3 being the most selective and performant in methanation at 673 K. In at least partial agreement, Hatzisymeon et al. [40] reported the following sequence of activity: Ni/CeO_2 > Ni/Y_2O_3–stabilized ZrO_2 > Ni/Al_2O_3 > Ni/TiO_2, all with 5 wt% Ni. These authors attribute the trend to the decreasing particle size of Ni metal particles. According to Ma et al. [41], the CO_2 methanation activity order for 5 wt% nickel catalysts on relatively low surface area supports is Ni/CeO_2 > Ni/Al_2O_3 > Ni/TiO_2 > Ni/ZrO_2. According to Gac et al. [42], the activity trend for 10–40 wt% Ni-supported catalysts is Ni/CeO_2 > Ni/ZrO_2 > Ni/Al_2O_3, all with very high methane selectivity. However, these authors underline that Al_2O_3-supported catalysts have the highest resistance against sintering. Lee et al. [43] reported the following activity trend: $Ni/CeO_2 \approx Ni/Y_2O_3$ > Ni/Al_2O_3 > Ni/TiO_2. These authors suggest that the reducibility of both metal and support at low temperatures, strong metal–support interaction, and small Ni particle size are important factors for low-temperature CO_2 methanation. Li et al. [44] reported the activity scale of Ni/CeO_2 > Ni/TiO_2 > Ni/SiO_2, with additional lower selectivity to methane for the Ni/SiO_2 catalyst, attributed to the absence of strong metal–support interaction.

3.2.1. Ni/SiO_2 Catalysts

As it is well known, amorphous silicas are largely covalent supports [45] which are usually supposed to be essentially non-dispersive with respect to other more ionic materials. Depending on the preparation method and type of materials, amorphous silicas have high morphological stability towards sintering and loss of surface area up to 873 K or more [46,47]. Silica is active in reversible adsorption, including of CO_2, with an important role of surface silanol groups as hydrogen bond donors [48], but without any Lewis acidity and basicity [49]. This is the reason for poor dispersing ability towards supported phases, as well as for poor adsorption of CO_2 without the formation of carbonate-like species.

Preparations of Ni/SiO_2 catalysts have been described by several authors. In general, it has been found that supporting nickel salts on amorphous silica followed by calcination gives rise to segregated NiO particles, although quite a small part of Ni^{2+} can be highly dispersed on ion exchange sites, i.e., exchanging protons in silanol group nests [50–52]. After reduction, such Ni/SiO_2 catalysts usually mainly present large Ni metal particles with poor dispersion [53] and poor interaction with the support, although the copresence of dispersed unreduced nickel has also been reported [52]. Stability towards sintering of the Ni/SiO_2 catalyst is limited [27], although the use of meso/microporous silica supports and opportune preparation methods can improve it [54].

The CO_2 hydrogenation reaction over Ni/SiO_2 catalysts has been the object of several studies. According to Gac et al. [55], small particles (d = 15.8 nm) of nickel on silica can show very high catalytic activity and selectivity to methane at low temperatures, while selectivity to CO increases with increased particle size and reaction temperature above

673 K. Wu et al. [56] reported a different result, showing that low-loading (0.5 wt% Ni/SiO_2) catalysts essentially work as a rWGS catalyst while high-loading and high particle size samples (10% Ni/SiO_2) are effective methanation catalysts. Galhardo et al. [57] reported high selectivity to CO for 15 wt% Ni/SiO_2 at both low and high temperatures, while near 673 K selectivity to methane is slightly higher than that to CO. These authors report data suggesting that the formation of carbon deposits on Ni metal particles produces Ni carbide species favoring the rWGS activity and deactivating methanation. Li et al. [44] reported lower methane selectivity for Ni/SiO_2 with respect to other supported Ni catalysts. Chen et al. [58] investigated CO_2 hydrogenation on Ni nanoparticles supported on surface-modified, cage-type mesoporous silica at 773 K, observing high selectivity to CO and low selectivity to methane. Riani et al. [52] reported that low-loading Ni/SiO_2 catalysts with particle sizes < 20 nm showed high selectivity to CO and moderate activity for the rWGS reaction, likely mainly due to nickel species dispersed in silica exchange sites, as evidenced by visible spectroscopy. The same authors reported that high-loading Ni/SiO_2 catalysts with particle size ~ 100 nm show both methanation and rWGS activity, but there is evident short-term deactivation for methanation (see the decreased methane yield in the decreasing temperature steps at the right of Figure 3), attributed to large, segregated Ni metal particles, covered by a carbon veil.

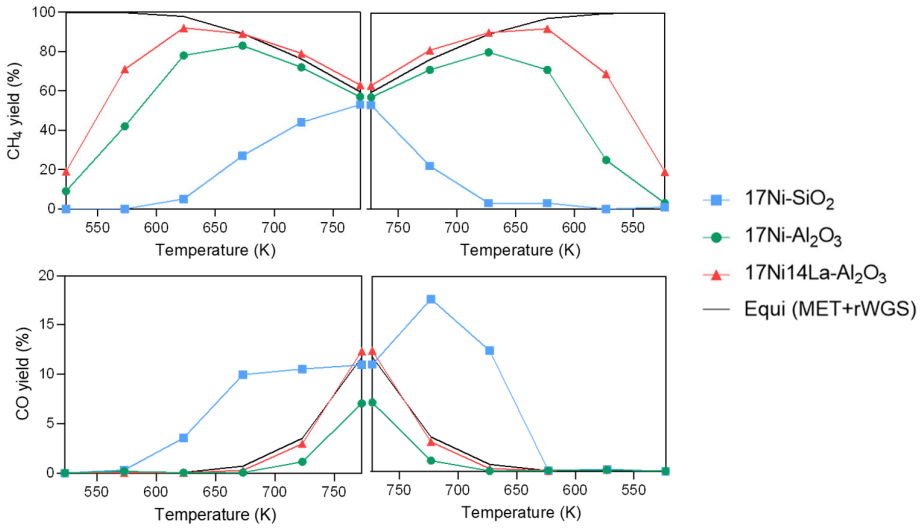

Figure 3. Methane yield and CO yield upon CO_2 hydrogenation over 17 wt% NiO (fresh catalyst) on pure amorphous silica (17Ni-SiO_2), on pure γ-Al_2O_3 (17Ni-Al_2O_3), and on 17 wt% La_2O_3-83 wt% γ-Al_2O_3. Feed 6 vol% CO_2, 30 vol% H_2, N_2 balance, and GHSV 55,000 h^{-1}. Modified from refs. [52,59].

Hao et al. [35] reported low activity for methanation and high activation energy (125 kJ/mol) for Ni/SiO_2 when compared with Ni/CeO_2 (E_{act} near 100 kJ/mol). Guo et al. [60] compared the methanation activity of different 10 wt% nickel catalysts supported on amorphous and mesoporous silica (SBA-15-type and MCM-41-type), showing that they have selectivity to methane approaching 100%, Ni/MCM-41 being definitely less active. In contrast, Bakariza et al. [61] found 15 wt% Ni/MCM-41 more active than Ni/SBA-15. Aziz et al. [62] reported high methanation activity and selectivity for 5% Ni/SiO_2 materials, with better performances when using sol–gel prepared mesostructured silica nanoparticles. Yang et al. [63] reported near-equilibrium conversion with 92% methane selectivity on a Ni/MCM-41 silica catalyst, whose activity is improved by zirconium doping. Vogt et al. [64] reported high selectivity to methane for a Ni/SiO_2 catalyst with 6 nm Ni particle size but lower selectivity, decreasing with time on stream, for methane for a Ni/SiO_2 catalyst with 1.8 nm Ni particle size. Zhu et al. [65] emphasized the progressive deactivation of a 20 wt% Ni/SiO_2 catalyst in a 30 h time on stream experiment. However, they also reported a significant increase in activity, selectivity to methane, and stability by further adding, in a

second step, additional silica, alumina, or zirconia over Ni/SiO_2. Guo and Lu [66] reported that co-impregnation of 1 wt% magnesium improves the activity and stability of 10% Ni/SiO_2, but the addition of more Mg results in lower activity and selectivity to methane.

3.2.2. Ni/Al_2O_3 Catalysts

In contrast to silica, spinel-type aluminas are considered to be ionic solids with high surface, Lewis acidity and basicity, and a strong ability to disperse supported species [67,68]. Thus, Ni dispersion on alumina is very high. Impregnation of γ-Al_2O_3 with Ni salts followed by calcination results in the formation of a $NiAl_2O_4$-like surface layer which is hardly reducible, forming, upon reduction, very small Ni metal clusters [69] which are very selective for CO_2 methanation [52,70], as evident from Figure 3. Instead, even at a high Ni loading, the formation of bulk $NiAl_2O_4$ does not occur until at least 873 K, given how the reaction between NiO and γ-Al_2O_3 is still slow and incomplete even at 1273 K [71]. However, the surface spinel layer stabilizes the Ni/γ-Al_2O_3 catalysts up to high temperatures [72], preventing bulk transformation and loss of surface area.

Surface characterization studies performed by IR spectroscopy of adsorbed CO allowed for the distinguishing of three types of surface Ni metal sites depending on Ni loading on reduced Ni-γ-Al_2O_3. For a low Ni loading, nearly isolated metal sites are able to adsorb CO in the form of polycarbonyls; at medium loadings, small nickel metal particles adsorb CO on-top (terminal carbonyls) only, and at higher coverages, larger metal particles adsorb CO also as bridging species [73].

In their screening work, among oxide-supported nickel catalysts, Muroyama et al. [39] found Ni/Al_2O_3 to be not very active at low temperatures (473–523 K) with respect to other oxide-supported Ni catalysts, but to be the most performant and selective to methane at 673 K. In an early study, Van Herwijnen et al. [74] reported a kinetic study of methanation of diluted CO_2 (1.4 vol%) in hydrogen, over 33.6 wt% NiO/γ-Al_2O_3 at 473–503 K, with full conversion at sufficiently high contact times already at 500 K at atmospheric pressure. For γ-alumina supports with 180–220 m^2/g, the best activity and selectivity are reported for catalysts with 15–25 wt% Ni [75,76], which roughly corresponds to the coverage of the support by a "geometric monolayer" of surface Ni aluminate species, while at a lower loading, both activity and selectivity decrease in favor of rWGS activity to CO. Otherwise, at an even higher loading, where larger but still strongly support-bonded Ni metal particles are formed, activity decreases, but deactivation is significant, while high selectivity is usually retained [77].

On the other hand, Ni-Al_2O_3 catalysts prepared by coprecipitation, such as by coprecipitated Ni-Al hydrotalcite, were reported to be definitely more active and more selective than impregnated Ni/γ-Al_2O_3 at medium-low loadings [78], but may be less active and selective at a near monolayer loading [75]. On the other hand, coprecipitated catalysts with very high Ni loadings (50–90 wt% Ni) were reported by Beierlein [77] to be definitely more active in methanation and stable than high-loading samples (>30 wt% Ni) produced by impregnation. These authors attribute this activity trend to the effect of higher nickel surface area. Indeed, when working with Ni-Al hydrotalcite, the Ni loading is usually very high. When working with a catalyst with a Ni/Al atomic ratio = 3, high selectivity to CO was found at low contact time, with methane selectivity increasing with increasing contact time [79].

3.2.3. Ni/CeO_2 Catalysts

Most authors of screening papers report ceria as the best oxide support for nickel catalysts used in CO_2 methanation. Hao et al. [35] reported excellent activity and near 100% methane selectivity over 7.5% Ni/CeO_2 with 25 m^2/g surface area, although the Turn Over Frequency increases by decreasing particle size as a result of decreasing loading. Methanation activity is already significant at 498 K with near 100% selectivity. Similarly, Bian et al. [80] reported activity already in the 473–523 K range for Ni/CeO_2 with a near 100% methane selectivity, which somehow depended on ceria particle morphologies: Ni

on ceria nanorods appeared to be more active than Ni on ceria nanocubes. Using ceria nanorods, Varvoutis et al. [32] showed high activity already in the 473–573 K range and equilibrium conversion above 623 K with total methane selectivity for samples with 8 to 33% Ni/CeO_2 (S_{BET} 72 to 51 m^2/g by increasing loading). On the other hand, low-loading Ni/CeO_2, with 1–2% nickel, are reported to work as excellent catalysts for the competitive reverse water gas shift reaction to CO [81]. The role of the preparation method has also been emphasized by several authors: Ye et al. [82] reported much higher activity and selectivity of sol–gel prepared Ni/CeO_2 than from an analogous catalyst produced by impregnation. As a key for explaining the best performances of Ni/CeO_2, the role of the partial reducibility of CeO_2, with the detection of Ce^{3+} ions, has been emphasized [83]. Indeed, among typical oxide carriers, ceria is the most reducible, and also has the ability to absorb hydrogen-forming bulk and surface hydride species [84]. In fact, it has been reported that the Ni/CeO_2 system is quite an unstable one, with the ability to dissolve Ni^{2+} ions in the bulk at higher temperatures and longer times [85]. It is, in fact, known that NiO can dissolve in CeO_2 in significant amounts, forming a solid solution with a fluorite structure [86,87], at least for small particle size nanomaterials. A similar deactivation phenomenon with loss of metal surface area is reported, e.g., for Pd/CeO_2 for the Water Gas shift reaction [88].

In their review, Xie et al. [89] summarized recent attempts to further improve Ni/CeO_2 catalysts for CO_2 methanation by modifying the preparation method (constructing more efficient structures and producing more efficient morphologies) and adding additional components, such as alkali, alkali–metal, and rare earth oxides and by alloying Ni with other transition metals. According to these authors, from a practical industrial point of view, challenges remain in developing a durable and low-cost CeO_2-based methanation catalyst with considerable low-temperature activity.

3.2.4. Ni/ZrO_2 Catalysts

As shown above, most screening studies report high methanation activity for Ni/ZrO_2. Chen et al. [90] investigated the activity of 15 wt% Ni/ZrO_2 catalysts with predominant monoclinic or tetragonal zirconia support: the monoclinic sample showed lower initial conversion temperature (down to 358 K) and higher basicity than the tetragonal one, both being very selective to methane formation, but with a slight selectivity decrease above 623 K. A similar result was reported by Jia et al. [91] for a 10 wt% Ni/ZrO_2 monoclinic + tetragonal zirconia support. Tan et al. [92] used a monoclinic + tetragonal zirconia support with a surface area of 96.6 m^2/g to prepare a series of Ni/ZrO_2 catalysts. While all catalysts showed selectivity to methane near 100%, the most active appeared to be that with a 6 wt% Ni loading. According to these authors, the intrinsic activity of the catalyst is related to the Ni dispersion and the size of metallic Ni; thus, excellent activity was obtained with highly dispersed particles. According to Vargas et al. [93], really highly dispersed 1 wt% Ni/m-ZrO_2 prepared by ultrasound-assisted synthesis is very active and selective in methanation of CO_2. Ma et al. confirmed the high activity of Ni/m-ZrO_2, more active than a catalyst based on cubic zirconia [94], attributing high activity to the high local electron density of nickel sites. Zhao et al. [95] compared the activities of different 15 wt% Ni/ZrO_2 catalysts produced by combustion with different combustion compounds with a sample produced by impregnation of a mainly monoclinic ZrO_2 support. The catalyst produced by the urea combustion method (resulting in being tetragonal) was reported to be the most active and stable, although, in the 573–773 K range, the impregnated sample was reported to be even more selective to methane. Concerns about the use of Ni/ZrO_2 catalytic materials is due to the potential of NiO to enter monoclinic, tetragonal, and cubic zirconia phases forming solid solutions [96,97] which influence the solid state chemistry of zirconia, apparently favoring the metastable tetragonal phase.

3.2.5. Nickel Catalysts Supported on Other Rare Earth Oxides

In a recent review, Spennati et al. [98] emphasized the role of rare earth oxides in the composition of Ni-based catalysts for CO_2 methanation. According to the screening work of Muroyama et al. [39], where pure support effect has been considered for 10 wt% Ni/oxide catalysts, Ni/Y_2O_3 and, to a lesser extent, Ni/Sm_2O_3, show the highest methanation activities at 523 K, although they lose methane selectivity above 573 K in favor of CO. Thus, the methanation activity of Ni/Y_2O_3 is closely similar to that of Ni/Al_2O_3 and Ni/ZrO_2 at 623 K. Other screening studies confirm the high activity of Ni/Y_2O_3, but no more than Ni/CeO_2 [43]. Li et al. [99] confirmed the very high methanation activity of 10 wt% Ni/Y_2O_3, if prepared in the presence of large amounts of citric acid in particular. Ni/Sm_2O_3 catalysts were also reported as interesting, with high low-temperature activity and almost total selectivity to methane, mainly when the sample is highly charged (63 wt% Ni) [100], with a slight deactivation attributed to carbonate formation.

Relatively high-loading Ni/La_2O_3 catalysts [101] are reported to be selective in the methanation of CO_2, while low-loading Ni/La_2O_3 appear to work as rWGS catalysts with high CO selectivity [102]. However, studies report that La_2O_3 is unstable in reaction conditions, suffering from carbonation or hydration with the formation of oxycarbonate and hydroxide production [103], respectively. On the other hand, 10 wt% Ni supported on the oxycarbonate $La_2O_2CO_3$ has been reported to display enhanced activity and stability with respect to Ni/La_2O_3 [104].

3.2.6. Other Ni/Oxide Catalysts

As commented before, most screening studies find a relatively low activity of Ni/TiO_2 with respect to other oxide-supported Ni catalysts. In their study, Unwiset et al. [105] found catalytic activity only above 573 K, increasing with the Ni loading, and high selectivity to methane for Ni/TiO_2-anatase samples. The XRD study of the catalysts shows that part of the nickel was incorporated in the anatase framework in the solid solution. When looking at solid state stability, the Ni/TiO_2-anatase system is considered to be quite an unstable one, since Ni^{2+} is a promoter of the anatase to rutile phase transformation [106] that usually also occurs at low temperatures with a significant loss of surface area. For example, the TiO_2 phase transformation was reported to affect the performance of the Ni/TiO_2 catalyst for biomass fast pyrolysis volatiles [107]. On the other hand, Messou et al. [108] found Ni/rutile more active than Ni/anatase, although Ni over a mixed phase support was even more active, showing some kind of synergism between the two TiO_2 phases. A few studies also report on the methanation activity of Ni/MgO catalysts [109,110], where high activity and selectivity to methane can also be found. It must be mentioned, however, that the full reciprocal solubility of NiO and MgO (which are isostructural) may represent an element of instability of the system if prepared by impregnation, or of limited efficiency per nickel atom if prepared by coprecipitation.

3.3. Effect of Addition of Doping with a Second Oxide on Ni/γ-Al_2O_3 and Ni/CeO_2

The data summarized above indicate that Ni/CeO_2 and $Ni/\gamma\text{-}Al_2O_3$ are likely the most attractive systems for CO_2 methanation: alumina is usually the preferred support by catalyst producers because of its moderate costs, its well-known chemistry, and its well-proven stability. On the other hand, $Ni\text{-}Al_2O_3$ catalysts are also already largely used in the industry for CO hydrogenation both to produce Synthetic Natural Gas and to remove CO and CO_2 from hydrogen and ammonia synthesis gas, as well as for several hydrogenations in the treatment of hydrocarbon streams [12]. Otherwise, Ni/CeO_2 seems to give more active catalysts, in particular at low temperatures. The use of CeO_2 is increasingly of interest in heterogeneous catalysis [111].

3.3.1. Effect of a Second Oxide Component on $Ni/\gamma\text{-}Al_2O_3$

Silica is a well-known stabilizer of the $\gamma\text{-}Al_2O_3$ against phase transition and surface area loss [49,112]. However, the addition of silica in small amounts to $\gamma\text{-}Al_2O_3$ shows a

slightly negative effect on CO_2 hydrogenation activity, although it may have a positive effect when applied in small amounts on the stability of the methanation activity [52]. Liang et al. reported on the effect of Na, K, Mg, Ca, Sc, Ti, V, Cr, Mn, Fe, Co, Ni, Cu, Zn, Zr, La, and Ce on the activity of Ni/γ-Al_2O_3 [113], observing that Zn only promotes methanation activity at low temperature, while Cr, Fe, Mn, La, Ce promote stability in prolonged CO_2 methanation experiments. In contrast, Cai et al. [114] reported a marked promotion effect of zirconia on 12 wt% Ni/γ-Al_2O_3, in particular when the 3 wt% ZrO_2/γ-Al_2O_3 carrier was prepared by the impregnation–precipitation method. In their recent review, Spennati et al. [98] emphasized the positive role of doping Ni/Al_2O_3 with rare earth oxide components. Ahmad et al. [115] reported the activity scale Pr > La > Gd > Ce > Eu for 12 wt% Ni/γ-Al_2O_3 doped with 5 wt% rare earth metal. Guilera et al. [116] co-impregnated alumina with nickel and Ce, La, Sm, Y, and Zr compounds and found La and Ce gave the best catalytic performance, while Sm and Zr showed a lower positive effect. Looking at the optimal amount of Ceria, Kim et al. [117] report maximum activation for methanation with 15 wt% CeO_2 for 15 wt% Ni/Al_2O_3 with 92 m^2/g surface area. As for the Ni/La_2O_3 –γ-Al_2O_3 system, Garbarino et al. [59] reported 14 wt% La_2O_3 as the best loading for 13.6 wt% Ni/γ-Al_2O_3 (17 wt% as NiO). In Figure 3, the positive effect of La_2O_3 addition to Ni/γ-Al_2O_3 is evident. This effect was in part attributed to the increased strength of absorption of CO_2 in the form of carbonate species over the La_2O_3-Al_2O_3 support, with respect to bicarbonate species on pure Al_2O_3. Riani et al. [118] reported later that the coaddition of silica and lanthana to Ni/γ-Al_2O_3 can give rise to catalysts with even higher low-temperature methanation activity. A catalyst obtained by a precursor with a weight composition of 16.7% NiO, 37.0% La_2O_3, 4.6% SiO_2, and 41.7% Al_2O_3 was found to be very active at 523 K.

Beierlein et al. [77] confirmed the negative effect of sodium impurities in the methanation activity and selectivity of Ni/γ-Al_2O_3. Potassium addition on Ni/γ-Al_2O_3 was reported by Gandara Loe et al. [119] to significantly increase CO selectivity, finally producing an excellent catalyst for rWGS at T > 873 K. As for alkali earth elements, Liang et al. [120] reported that Ba (1–5 wt% loading) doping of Ni/γ-Al_2O_3 results in a remarkable selectivity increase, while Sr is less effective and Mg and Ca enhance rWGS reaction, thus reducing methane selectivity. However, Garbarino et al. [121] reported that Ni/Ca-aluminate industrial methane steam reforming catalyst (18 wt% NiO in the catalyst precursor) has excellent activity and selectivity to methane, which are both decreased by 1.8 wt% K_2O doping. Garbarino et al. [122] found excellent low-temperature activity for Ca-doped 19 wt% Ni/γ-Al_2O_3, further enhanced by the addition of V_2O_5.

A very interesting point concerns the Ni/MgO-Al_2O_3 system, which can be prepared by coprecipitation starting from Ni-Mg-Al hydrotalcite-type double hydroxides. Liu et al. reported that Ni/MgAl catalysts (36.9 wt% Ni, (Ni + Mg)/Al = 2) exhibit outstanding performance in CO_2 methanation, compared with Ni/γ-Al_2O_3 and Ni/MgO [123], associated with a very small Ni metal particle size, allowing better low-temperature CO_2 methanation activity. Very high CO_2 methanation activity and selectivity, higher than that of Ni/γ-Al_2O_3, was recently reported by Fasolini et al. [124] for ex-hydrotalcite 27 wt% Ni/MgO-Al_2O_3.

Another element that has been reported as a good activator for methanation on Ni/γ-Al_2O_3 is manganese. Zhao et al. [125] reported maximum activation of 15 wt% Ni/γ-Al_2O_3 by adding 1.7 wt% Mn. These authors attributed the activation effect to the increased number of CO_2 adsorption sites, the improved Ni dispersion, and the weakened interactions between the nickel species and the support. In good agreement, Vrijburg et al. [126] reported significantly higher methanation rates and CH_4 selectivities for Mn-promoted Ni/γ-Al_2O_3. The optimal Mn/Ni atomic ratio was found to be 0.25, showing metallic Ni particles and small oxidic Mn^{2+} species. According to these authors, Mn addition improves Ni dispersion and enhances Ni^{2+} reducibility by weakening the interaction between the Ni-oxide precursor and the support. Wu et al. [127] reported on the excellent methanation activity of a catalyst with 20 wt% Ni/Al_2O_3-ZrO_2 doped with 6.7% Mn. All

these studies conclude that Mn oxide species are dispersed on the support surface, favoring nickel dispersion.

3.3.2. Effect of a Second Oxide Component on Ni/CeO_2

A number of studies reported on the further promotion of Ni/CeO_2 for CO_2 methanation. The use of CeO_2-ZrO_2 solid solutions is a common way to stabilize ceria. Pan et al. [128] found $Ni/Ce_{0.5}Zr_{0.5}O_2$ to definitely be more active than Ni/γ-Al_2O_3 and attributed to the stronger basicity of the $Ce_{0.5}Zr_{0.5}O_2$ support, having more and stronger CO_2 adsorption sites than γ-Al_2O_3. Looking at different CeO_2-ZrO_2 support compositions, Ullah et al. [129] found maximum activity for 5 wt% Ni catalysts when the support composition is $Ce_{0.7}Ni_{0.3}O_2$. A number of studies reported the promoting effect of rare earth ions on the activity of Ni/CeO_2, such as Eu^{3+} [130], Sm^{3+} [131], Y^{3+} [132], the couples La^{3+} -Sm^{3+}, La^{3+}-Pr^{3+}, and La^{3+} -Mg^{2+} [133], etc. Looking at the effect of alkali earth metals, Liu et al. [134] found an increase in the methanation activity of Ni/CeO_2 by adding Ca^{2+} and Mg^{2+}, with a more limited effect for Sr^{2+} and a deactivation effect for Ba^{2+}.

3.4. Effect of Alloying

Several studies report bimetallic Ni-based catalysts being more active than pure nickel ones in CO_2 methanation. This subject has been reviewed recently by Tsiotsias et al. [26]. The addition of small amounts of noble metals (Pt, Ru, Rh, Pd, and Re) to Ni/Al_2O_3 provides several advantages, such as excellent activity at low temperatures, high reducibility, and stability once oxidized [135], producing even new sites or by forming an alloy with nickel as evidenced for Ru and Pt or Pd, respectively. However, the use of very expensive noble metals to activate nickel may make sense only if they are added in extremely small amounts, due to their activity even at small loadings over oxide support. According to Pan et al. [136] the addition of 0.2 wt% Ru causes a 3-fold rate enhancement at low temperature for selective methanation of CO_2 relative to the monometallic 20 wt% Ni/CeO_2 and to 0.2 wt% Ru/CeO_2.

The use of less expensive transition metal to increase Ni activity seems to be more interesting. As already cited, according to Pandey [31], the moderate activity of pure nickel is significantly increased by the addition of small amounts of iron. For example, the addition of 1 wt% cobalt was reported to significantly increase the low-temperature activity of 15 wt% Ni/MgO-Al_2O_3 catalysts [137]. Similarly, the addition of 4.7 wt% iron significantly increases the low-temperature activity of a 20 wt% Ni/MgO-Al_2O_3 catalyst [138]. According to Xu et al. [139], the additions of Fe, Co, and, to a lower extent, Mn on $Ni/Ce_{0.8}Zr_{0.2}$ enhance activity, while copper addition decreases both activity and selectivity to CH_4. Over low-loading Ni/La_2O_3, copper addition increases rWGS activity and selectivity to CO [102].

4. Discussion

The data summarized above show that, essentially, all Ni-containing catalysts found activity in CO_2 hydrogenation. In Table 1, the most relevant criteria for selecting optimal Ni-based CO_2 methanation catalysts are proposed. Catalysts where most of the nickel species remain unreduced, because they strongly interact with the oxide support, usually have predominant rWGS activity to CO, while those where sufficient nickel can be reduced to the metallic state have at least good initial activity to methanation. It seems that good and stable methanation activity is associated mainly with very small nickel metal particles associated with very high nickel dispersion, which can be stabilized mainly on ionic oxides. In fact, for large particle Ni catalysts, fast deactivation by carbon deposition is usually observed, which may also result in switching toward higher CO selectivity by rWGS activity, likely due to carbon or nickel carbide species.

Table 1. Proposed criteria for selecting optimal Ni-based CO_2 methanation catalysts.

Nickel state	reduced
Nickel particle size	very small
Support type	ionic, dispersing
	not dissolving Ni
Nickel loading	near a "monolayer" on the support surface
Support surface chemistry	containing some basicity
Additive(s)	favoring nickel dispersion
	producing medium basicity
	activating nickel by electronic effects
	alloying nickel

Methanation occurring on unsupported Ni particles and Ni/SiO_2 should fully occur at the nickel metal surface, where carbide or carbon intermediates are reasonably formed and active in methanation [140]. However, mechanisms via oxygenate intermediates (carboxylate, carbonate, formate, formyl, and methoxy) can also occur at nickel surfaces [141]. On ionic oxides, where CO_2 adsorbs and forms different types of carbonate and bicarbonate species [23], a more important role of the support in the methanation mechanism is plausible [142].

Very high low-temperature methanation activity is obtained on small Ni metal particles supported on semiconducting and slightly reducible metal oxides characterized by medium surface basicity, such as, in particular, for Ni/CeO_2. On the other hand, it seems also quite evident that the addition of basic, semiconducting, and moderately reducible components to alumina (a non-conducting, non-reducible, and mainly acidic support) is sufficient to significantly increase the methanation activity at 473–523 K, up to values comparable to those obtained with (doped) Ni/CeO_2, and with Ru/Al_2O_3 as well. Such components to be added to alumina support include, e.g., cerium or manganese oxides.

The activating effect of such an intermediate level of basicity is usually attributed to the resulting ability of the support to adsorb CO_2 in the form of carbonate species that, thanks to the spillover of hydrogen from nickel metal particles, is at the origin of a oxygenate intermediate-based hydrogenation mechanism [143]. For example, the activating effect of the addition of La_2O_3 to $Ni/\gamma\text{-}Al_2O_3$ has been attributed in part to the increased strength in the adsorption of CO_2 [59]; as shown in Figure 4, the adsorbed species of CO_2 are fully modified.

On $\gamma\text{-}Al_2O_3$, two slightly different forms of bicarbonates are observed (Figure 4, bands at 1644 cm^{-1}; O-C-O asymmetric stretching, 1484, 1442 cm^{-1}, two different O-C-O symmetric stretchings, 1236 cm^{-1}, COH deformation mode), whose band decreased by the addition of La_2O_3 until almost disappearing, while bands due to two forms of carbonates are formed (COx stretchings at 1680 and 1380 cm^{-1}, likely bridging carbonates, and at 1540 and 1435 cm^{-1}, likely monodentate carbonates). However, slight effects in modifying the electronic properties of Ni metal particles by increasing support basicity as well as semiconducting or redox species cannot be excluded [59].

As shown above, the addition of small amounts of another metal, e.g., cobalt or ruthenium, can also produce a significant increase in activity at low temperatures.

On the other hand, to develop industrial catalysts, besides (initial) activity, other factors must be considered and are even more relevant. In their work concerning high-temperature methanation of CO-rich syngases, Nguyen et al. [13] reported that catalysts must be stable against metal particles and support sintering, formation of carbon and gum residues, as well as the formation of nickel tetracarbonyl. Such a volatile compound can favor Ni particle growth through its formation and decomposition. The need to avoid $Ni(CO)_4$ formation drives the limiting of nickel loading and the use of sufficiently high

reaction temperatures, e.g., >573 K, where such gaseous compounds cannot form. Thus, for this reason, the very low-temperature activity of the catalyst cannot be so relevant.

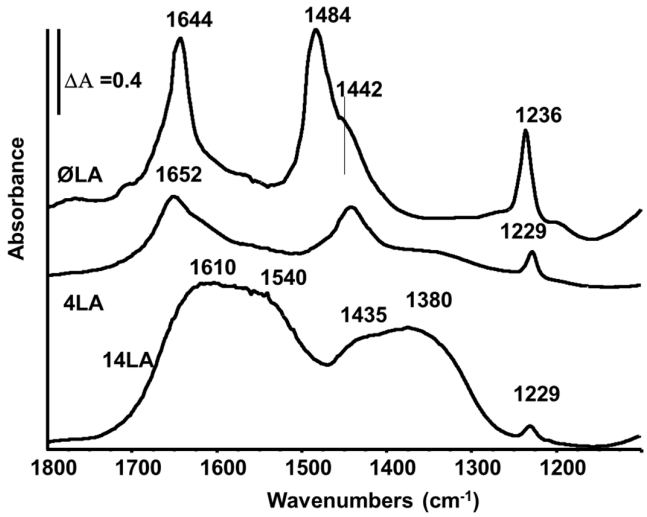

Figure 4. IR spectra of the adsorbed species after CO_2 adsorption on γ-Al_2O_3, 4 wt% La_2O_3-Al_2O_3, and 14 wt% La_2O_3-Al_2O_3, modified from Ref. [59].

It seems that the limitation of the formation of carbon residue and gum can be obtained using catalysts allowing the production of small to very small nickel metal particles in reaction conditions. This is apparently obtained using high-dispersing ionic oxide supports and a moderate loading of nickel.

Another point is certainly the solid state stability of the support and its reactivity towards nickel species. In fact, most metal oxides allow solubility of Ni^{2+}, forming mixed oxides. The penetration of nickel in the bulk of the support, with the help of the slight oxidizing properties of the reactant CO_2 and of the product H_2O, would result in the consumption of the active phase (metallic nickel) and in the deterioration of the morphological properties of the support. From this point of view, γ-Al_2O_3 seems to be optimal, taking into account that it tends to be covered by a $NiAl_2O_4$-like surface layer upon the preparation of the catalyst that protects the bulk from further Ni penetration. On the other hand, for decades, the use of Ni/Al_2O_3 catalysts in several other hydrogenation processes in relevant industrial conditions has been a confirmation of the stability of this system. In fact, as reported recently by Spennati et al., commercial Ni catalysts for CO_x methanation seem to be exclusively based on Ni/Al_2O_3 [98]. This might be due to its cheapness and well-known chemistry of alumina, coupled with its commercial availability, stability in mild conditions, and versatility, which make it preferred by the industry, e.g., as hydrotreating catalysts, as reported years ago [144]. It must also be taken into consideration that even though coprecipitated Ni/Al_2O_3-based catalysts may be a little more active than impregnated ones at least at initial steps, the less complete use of nickel in coprecipitated samples and the likely simpler preparation of catalysts by co-impregnation of commercial alumina with nickel and dopants can have advantages (also from the environmental point of view) with respect to more complex coprecipitation procedures.

5. Conclusions

A detailed analysis of the scientific literature data concerning catalysts for CO_2 methanation allowed us to evidence the main features needed for such an application. It seems that the necessary features of the best-performing oxide-supported nickel catalyst for CO_2 methanation are as follows:

1. The use of an ionic support that allows good nickel dispersion, resulting in very small nickel metal particles. Such small metal particles would be very active toward methanation and would not produce many carbon residues and gums;

2. The use of a support and/or surface additives that produce a medium basicity, allowing a medium-strong adsorption of CO_2;
3. A medium nickel loading, which allows the free support's geometric surface to be covered with optimal density by small nickel metal particles, without the production of larger Ni crystals and allows sufficient active sites for CO_2 adsorption on the support surface;
4. Working at temperatures where $Ni(CO)_4$ formation is impossible (e.g., >573 K).

Taking into account the already significant use of Ni/Al_2O_3 systems for catalytic hydrogenations, its ascertained long-term stability, and the common use of γ-alumina as a catalyst support, the application of 15–20 wt% nickel over a typical γ-Al_2O_3 (200 m^2/g) with small amounts of slightly reducible and basic promoters, such as Ce^{4+} and Mn^{n+}, or/and of simply mild basic components, such as Mg^{2+}, and maybe small amounts of an alloying metal, such as cobalt or iron, can be recommended. The most likely alternatives are based on Ni/CeO_2 with additives, whose long-term stability, however, should be verified.

Author Contributions: Conceptualization, methodology, and writing—review and editing, G.B., E.S., P.R. and G.G. All authors have read and agreed to the published version of the manuscript.

Funding: This research was partially funded under the National Recovery and Resilience Plan (NRRP), Mission 4 Component 2 Investment 1.3—Call for tender No. 1561 of 11.10.2022 of Ministero dell'Uni-versità e della Ricerca (MUR); funded by the European Union—NextGenerationEU Project title "Network 4 Energy Sustainable Transition—NEST" (Project code PE0000021).

Data Availability Statement: No new data were created or analyzed in this review study.

Conflicts of Interest: The authors declare no conflict of interest.

References

1. Götz, M.; Lefebvre, J.; Mörs, F.; Koch, A.M.; Graf, F.; Bajohr, S.; Reimert, R.; Kolb, R. Renewable Power-to-Gas: A Technological and Economic Review. *Renew. Energy* **2016**, *85*, 1371–1390. [CrossRef]
2. Vega Puga, E.; Moumin, G.; Neumann, N.C.; Roeb, M.; Ardone, A.; Sattler, C. Holistic View on Synthetic Natural Gas Production: A Technical, Economic and Environmental Analysis. *Energies* **2022**, *15*, 1608. [CrossRef]
3. Tripodi, A.; Conte, F.; Rossetti, I. Carbon Dioxide Methanation: Design of a Fully Integrated Plant. *Energy Fuels* **2020**, *34*, 7242–7256. [CrossRef]
4. Bolt, A.; Dincer, I.; Agelin-Chaab, M. A critical review of synthetic natural gas production techniques and technologies. *J. Nat. Gas Sci. Eng.* **2020**, *84*, 103670. [CrossRef]
5. Mazheika, A.; Wang, Y.G.; Valero, R.; Viñes, F.; Illas, F.; Ghiringhelli, L.M.; Levchenko, S.V.; Scheffler, M. Artificial-intelligence-driven discovery of catalyst genes with application to CO_2 activation on semiconductor oxides. *Nat. Commun.* **2022**, *13*, 419. [CrossRef] [PubMed]
6. Gao, J.; Wang, Y.; Ping, Y.; Hu, D.; Xu, G.; Gu, F.; Su, F. A thermodynamic analysis of methanation reactions of carbon oxides for the production of synthetic natural gas. *RSC Adv.* **2012**, *2*, 2358–2368. [CrossRef]
7. Stangeland, K.; Kalai, D.; Li, H.; Yu, Z. CO_2 methanation: The effect of catalysts and reaction conditions. *Energy Proced.* **2017**, *105*, 2022–2027. [CrossRef]
8. Bertucco, A.; Fermeglia, M. 50 years of Soave Equation of State (SRK): A source of inspiration for chemical engineers. *Fluid Phase Equilibria* **2023**, *566*, 113678. [CrossRef]
9. Torrente-Murciano, L.; Mattia, D.; Jones, M.D.; Plucinski, P.K. Formation of hydrocarbons via CO_2 hydrogenation—A thermodynamic Study. *J. CO_2 Util.* **2014**, *6*, 34–39. [CrossRef]
10. Schmider, D.; Maier, L.; Deutschmann, O. Reaction Kinetics of CO and CO_2 Methanation over Nickel. *Ind. Eng. Chem. Res.* **2021**, *60*, 5792–5805. [CrossRef]
11. Liao, L.; Chen, L.; Ye, R.P.; Tang, X.; Liu, J. Robust nickel silicate catalysts with high Ni loading for CO_2 methanation. *Chem. Asian J.* **2021**, *16*, 678–689. [CrossRef] [PubMed]
12. Busca, G. Metal catalysts in hydrogenation and dehydrogenation reactions. In *Heterogeneous Catalytic Materials*; Busca, G., Ed.; Elsevier: Amsterdam, The Netherlands, 2014; pp. 297–343.
13. Nguyen, T.T.M.; Wissing, L.; Skjøth-Rasmussen, M.S. High temperature methanation: Catalyst considerations. *Catal. Today* **2013**, *215*, 233–238. [CrossRef]
14. Frontera, P.; Macario, A.; Ferraro, M.; Antonucci, P.L. Supported Catalysts for CO_2 Methanation: A Review. *Catalysts* **2017**, *7*, 59. [CrossRef]
15. Ashok, J.; Pati, P.; Hongmanorom, P.; Tianxi, Z.; Junmei, C.; Kawi, S. A review of recent catalyst advances in CO_2 methanation processes. *Catal. Today* **2020**, *356*, 471–489. [CrossRef]

16. Tan, C.H.; Nomanbhay, S.; Shamsuddin, A.H.; Park, Y.K.; Hernández-Cocoletzi, H.; Show, P.L. Current Developments in Catalytic Methanation of Carbon Dioxide—A Review. *Front. Energy Res.* **2022**, *9*, 795423. [CrossRef]
17. Pham, C.Q.; Bahari, M.B.; Kumar, P.S.; Ahmed, S.F.; Xiao, L.; Kumar, S.; Qazaq, A.S.; Siang, T.J.; Tran, H.T.; Islam, A.; et al. Carbon dioxide methanation on heterogeneous catalysts: A review. *Environ. Chem. Lett.* **2022**, *20*, 3613–3630. [CrossRef]
18. Abild-Pedersen, F.; Andersson, M.P. CO adsorption energies on metals with correction for high coordination adsorption sites—A density functional study. *Surf. Sci.* **2007**, *601*, 1747–1753. [CrossRef]
19. Goldberger, W.M.; Othmer, D.F. Kinetics of Nickel Carbonyl Formation. *Ind. Eng. Chem. Process Des. Dev.* **1963**, *2*, 202–209. [CrossRef]
20. Calatayud, M.; Markovits, A.; Menetrey, M.; Mguig, B.; Minot, C. Adsorption on perfect and reduced surfaces of metal oxides. *Catal. Today* **2003**, *85*, 125–143. [CrossRef]
21. Burghaus, U. Surface chemistry of CO_2—Adsorption of carbon dioxide on clean surfaces at ultrahigh vacuum. *Progr. Surf. Sci.* **2014**, *89*, 161–217. [CrossRef]
22. Monachino, E.; Greiner, M.; Knop-Gericke, A.; Schlögl, R.; Dri, C.; Vesselli, E.; Comelli, G. Reactivity of Carbon Dioxide on Nickel: Role of CO in the Competing Interplay between Oxygen and Graphene. *J. Phys. Chem. Lett.* **2014**, *5*, 1929–1934. [CrossRef] [PubMed]
23. Busca, G.; Lorenzelli, V. Infrared spectroscopic identification of species arising from reactive adsorption of carbon oxides on metal oxide surfaces. *Mater. Chem.* **1982**, *7*, 89–126. [CrossRef]
24. Ramis, G.; Busca, G.; Lorenzelli, V. Low-temperature CO_2 adsorption on metal oxides: Spectroscopic characterization of some weakly adsorbed species. *Mater. Chem.* **1991**, *29*, 425–435. [CrossRef]
25. Strucks, P.; Failing, L.; Kaluza, S. A Short Review on Ni-Catalyzed Methanation of CO_2: Reaction Mechanism, Catalyst Deactivation, Dynamic Operation. *Chem. Ing. Tech.* **2021**, *93*, 1526–1536. [CrossRef]
26. Tsiotsias, A.I.; Charisiou, N.D.; Yentekakis, I.V.; Goula, M.A. Bimetallic Ni-Based Catalysts for CO2 Methanation: A Review. *Nanomaterials* **2021**, *11*, 28. [CrossRef] [PubMed]
27. Abboud, M.; Alnefaie, R.; Alhanash, A. Unsupported and silica-supported nickel nanoparticles: Synthesis and application in catalysis. *J. Nanopart. Res.* **2022**, *24*, 21. [CrossRef]
28. Teng, C.; He, J.; Zhu, L.; Ren, L.; Chen, J.; Hong, M.; Wang, Y. Fabrication and Characterization of Monodisperse Magnetic Porous Nickel Microspheres as Novel Catalysts Nanoscale. *Res. Lett.* **2015**, *10*, 384. [CrossRef]
29. Lucchini, M.A.; Testino, A.; Ludwig, C.; Kambolis, A.; El-Kazzi, A.; Cervellino, A.; Riani, P.; Canepa, F. Continuous synthesis of nickel nanopowders: Characterization, process optimization, and catalytic properties. *Appl. Catal. B Environ.* **2014**, *156–157*, 404–415. [CrossRef]
30. Garbarino, G.; Riani, P.; Magistri, L.; Busca, G. A study of the methanation of carbon dioxide on Ni/Al_2O_3 catalysts at atmospheric pressure. *Int. J. Hydrogen Energy* **2014**, *39*, 11557–11565. [CrossRef]
31. Pandey, D.; Ray, K.; Bhardwaj, R.; Bojja, S.; Chary, K.V.R.; Deo, G. Promotion of unsupported nickel catalyst using iron for CO_2 methanation. *Int. J. Hydrogen Energy* **2018**, *43*, 4987–5000. [CrossRef]
32. Varvoutis, G.; Lykaki, M.; Stefa, S.; Binas, V.; Marnellos, G.E.; Konsolakis, M. Deciphering the role of Ni particle size and nickel-ceria interfacial perimeter in the low-temperature CO_2 methanation reaction over remarkably active Ni/CeO_2 nanorods. *Appl. Catal. B Environ.* **2021**, *29*, 120401. [CrossRef]
33. Kristiani, A.; Takeishi, K. CO_2 methanation over nickel-based catalyst supported on yttria-stabilized zirconia. *Catal. Comm.* **2022**, *165*, 106435. [CrossRef]
34. Lee, G.D.; Moon, M.J.; Park, J.H.; Park, S.S.; Hong, S.S. Korean, Raney Ni catalysts derived from different alloy precursors Part II. CO and CO_2 methanation activity. *Korean J. Chem. Eng.* **2005**, *22*, 541–546. [CrossRef]
35. Hao, Z.; Shen, J.; Lin, S.; Han, X.; Chang, X.; Liu, J.; Li, M.; Ma, X. Decoupling the effect of Ni particle size and surface oxygen deficiencies in CO_2 methanation over ceria supported Ni. *Appl. Catal. B* **2021**, *286*, 119922. [CrossRef]
36. Riani, P.; Garbarino, G.; Lucchini, M.A.; Canepa, F.; Busca, G. Unsupported versus alumina-supported Ni nanoparticles as catalysts for steam/ethanol conversion and CO_2 methanation. *J. Mol. Catal. A Chem.* **2014**, *383–384*, 10–16. [CrossRef]
37. Riani, P.; Garbarino, G.; Infantes-Molina, A.; Rodríguez-Castellón, E.; Canepa, F.; Busca, G. Hydrogen from steam reforming of ethanol over cobalt nanoparticles: Effect of boron, impurities. *Appl. Catal. A Gen.* **2016**, *518*, 67–77. [CrossRef]
38. Lan, P.-W.; Wang, C.C.; Chen, C.Y. Enhancing the formation of nickel catalysts (111) crystal plane and CO_2 methanation reactivity by external magnetic field. *J. Taiwan Inst. Chem. Eng.* **2020**, *116*, 188–196. [CrossRef]
39. Muroyama, H.; Tsuda, Y.; Asakoshi, T.; Masitah, H.; Okanishi, T.; Matsui, T.; Eguchi, K. Carbon Dioxide Methanation over Ni Catalysts Supported on Various Metal Oxides. *J. Catal.* **2016**, *343*, 178–184. [CrossRef]
40. Hatzisymeon, M.; Petala, A.; Panagiotopoulou, P. Carbon Dioxide Hydrogenation over Supported Ni and Ru Catalysts. *Catal. Lett.* **2021**, *151*, 888–900. [CrossRef]
41. Ma, Y.; Liu, J.; Chu, M.; Yue, J.; Cui, Y.; Xu, G. Cooperation Between Active Metal and Basic Support in Ni-Based Catalyst for Low-Temperature CO_2 Methanation. *Catal. Lett.* **2020**, *150*, 1418–1426. [CrossRef]
42. Gac, W.; Zawadzki, W.; Rotko, M.; Greluk, M.; Słowik, G.; Kolb, G. Effects of support composition on the performance of nickel catalysts in CO_2 methanation reaction. *Catal. Today* **2020**, *357*, 468–482. [CrossRef]
43. Lee, Y.H.; Ahn, J.Y.; Nguyen, D.D.; Chang, S.W.; Kim, S.S.; Lee, S.M. Role of oxide support in Ni based catalysts for CO_2 methanation. *RSC Adv.* **2021**, *11*, 17648. [CrossRef] [PubMed]

44. Li, M.; Amari, H.; van Veen, A.C. Metal-oxide interaction enhanced CO_2 activation in methanation over ceria supported nickel nanocrystallites. *Appl. Catal. B Environ.* **2018**, *239*, 27–35. [CrossRef]
45. Busca, G. The surface acidity of solid oxides and its characterization by IR spectroscopic methods. An attempt at systematization. *Phys. Chem. Chem. Phys.* **1999**, *1*, 723–736. [CrossRef]
46. Wu, Y.; Wang, X.; Liu, L.; Zhang, Z.; Shen, J. Alumina-Doped Silica Aerogels for High-Temperature Thermal Insulation. *Gels* **2021**, *7*, 122. [CrossRef] [PubMed]
47. Feng, J.; Yan, Y.; Chen, D.; Ni, W.; Yang, J.; Ma, S.; Mo, W. Study of thermal stability of fumed silica based thermal insulating composites at high temperatures. *Compos. Part B* **2011**, *42*, 1821–1825. [CrossRef]
48. Busca, G. Location and Accessibility of Hydroxy Groups in Silico-aluminate Porous Materials as Studied by IR Spectroscopy. *Curr. Phys. Chem.* **2012**, *2*, 136–150. [CrossRef]
49. Busca, G. Catalytic materials based on silica and alumina: Structural features and generation of surface acidity. *Progr. Mat. Sci.* **2019**, *104*, 215–249. [CrossRef]
50. Mile, B.; Stirling, D.; Zammitt, M.A.; Lovell, A.; Webb, M. The location of nickel oxide and nickel in silica-supported catalysts: Two forms of "NiO" and the assignment of temperature-programmed reduction profiles. *J. Catal.* **1988**, *114*, 217–229. [CrossRef]
51. Bonneviot, L.; Legendre, O.; Kermarec, M.; Olivier, D.; Che, M. Characterization by UV-vis-NIR Reflectance Spectroscopy of the Exchange Sites of Nickel on Silica. *J. Coll. Interf. Sci.* **1990**, *134*, 534–547. [CrossRef]
52. Riani, P.; Spennati, E.; Villa Garcia, M.; Sanchez Escribano, V.; Busca, G.; Garbarino, G. Ni/Al_2O_3 catalysts for CO_2 methanation: Effect of silica and nickel loading. *Int. J. Hydrogen Energy* **2023**, *in press*. [CrossRef]
53. Xu, Y.; Du, X.; Li, J.; Wang, P.; Zhu, J.; Ge, F.; Zhou, J.; Song, M.; Zhu, W. A comparison of Al_2O_3 and SiO_2 supported Ni-based catalysts in their performance for the dry reforming of Methane. *J. Fuel. Chem. Technol.* **2019**, *47*, 199–208. [CrossRef]
54. Lucchini, M.A.; Testino, A.; Kambolis, A.; Proff, C.; Ludwig, C. Sintering and coking resistant core–shell microporous silica–nickel nanoparticles for CO methanation: Towards advanced catalysts production. *Appl. Catal. B Envir.* **2016**, *182*, 94–101. [CrossRef]
55. Gac, W.; Zawadzki, W.; Słowik, G.; Sienkiewicz, A.; Kierys, A. Nickel catalysts supported on silica microspheres for CO_2 methanation. *Micropor. Mesopor. Mat.* **2018**, *272*, 79–91. [CrossRef]
56. Wu, H.C.; Chang, Y.C.; Wu, J.H.; Lin, J.H.; Linc, I.K.; Chen, C.S. Methanation of CO_2 and reverse water gas shift reactions on Ni/SiO_2 catalysts: The influence of particle size on selectivity and reaction pathway. *Catal. Sci. Technol.* **2015**, *5*, 4154–4163. [CrossRef]
57. Galhardo, T.S.; Braga, A.H.; Arpini, B.H.; Szanyi, J.; Gonçalves, R.V.; Zornio, B.F.; Miranda, C.R.; Rossi, L.M. Optimizing Active Sites for High CO Selectivity during CO_2 Hydrogenation over Supported Nickel Catalysts. *J. Am. Chem. Soc.* **2021**, *143*, 4268–4280. [CrossRef]
58. Chen, C.S.; Budi, C.S.; Wu, H.C.; Saikia, S.; Kao, H.M. Size-Tunable Ni Nanoparticles Supported on Surface-Modified, Cage-Type Mesoporous Silica as Highly Active Catalysts for CO_2 Hydrogenation. *ACS Catal.* **2017**, *7*, 8367–8381. [CrossRef]
59. Garbarino, G.; Wang, C.; Cavattoni, T.; Finocchio, E.; Riani, P.; Flytzani-Stephanopoulos, M.; Busca, G. A study of Ni/La-Al_2O_3 catalysts: A competitive system for CO_2 Methanation. *Appl. Catal. B Environ.* **2019**, *248*, 286–297. [CrossRef]
60. Guo, X.; Traitangwong, A.; Hu, M.; Zuo, C.; Meeyoo, V.; Peng, Z.; Li, C. Carbon Dioxide Methanation over Nickel-Based Catalysts Supported on Various Mesoporous Materials. *Energy Fuels* **2018**, *32*, 3681–3689. [CrossRef]
61. Bacariza, M.C.; Graça, I.; Bebiano, S.S.; Lopes, J.M.; Henriques, C. Micro- and mesoporous supports for CO_2 methanation catalysts: A comparison between SBA-15, MCM-41 and USY zeolite. *Chem. Eng. Sci.* **2018**, *175*, 72–83. [CrossRef]
62. Aziz, A.A.; Jalil, A.A.; Triwahyono, S.; Mukti, R.R.; Taufiq-Yap, Y.H.; Sazegar, M.R. Highly active Ni-promoted mesostruc-tured silica nanoparticles for CO_2 methanation. *Appl. Catal. B Environ.* **2014**, *147*, 359–368. [CrossRef]
63. Yang, M.; Zhu, L.; Zhu, X.; Reubroycharoen, P.; Wang, S. CO_2 methanation over nickel-based catalysts supported on MCM-41 with in situ doping of zirconium. *J. CO_2 Util.* **2020**, *42*, 101304. [CrossRef]
64. Vogt, C.; Groeneveld, E.; Kamsma, G.; Nachtegaal, M.; Lu, L.; Kiely, C.J.; Berben, P.H.; Meirer, F.; Weckhuysen, B.M. Unravelling structure sensitivity in CO_2 hydrogenation over nickel. *Nat. Catal.* **2018**, *1*, 127–134. [CrossRef]
65. Zhu, P.; Chen, Q.; Yoneyama, Y.; Tsubaki, N. Nanoparticle modified Ni-based bimodal pore catalysts for enhanced CO_2 methanation. *RSC Adv.* **2014**, *4*, 64617. [CrossRef]
66. Guo, M.; Lu, G. The effect of impregnation strategy on structural characters and CO_2 methanation properties over MgO modified Ni/SiO_2 catalysts. *Catal. Commun.* **2014**, *54*, 55–60. [CrossRef]
67. Busca, G. The surface of transition aluminas. A critical Review. *Catal. Today* **2014**, *226*, 2–13. [CrossRef]
68. Busca, G. Structural, surface and catalytic properties of aluminas. *Adv. Catal.* **2014**, *57*, 319–404. [CrossRef]
69. Garbarino, G.; Chitsazan, S.; Phung, T.K.; Riani, P.; Busca, G. Preparation of supported catalysts: A study of the effect of small amounts of silica on Ni/Al_2O_3 catalysts. *Appl. Catal. A Gen.* **2015**, *505*, 86–97. [CrossRef]
70. Garbarino, G.; Bellotti, D.; Riani, P.; Magistri, L.; Busca, G. Methanation of carbon dioxide on Ru/Al_2O_3 and Ni/Al_2O_3 catalysts at atmospheric pressure: Catalysts activation, behaviour and stability. *Int. J. Hydrogen Energy* **2015**, *40*, 9171–9182. [CrossRef]
71. Li, C.Y.; Zhang, H.J.; Chen, Z.Q. Reaction between NiO and Al_2O_3 in NiO/-Al_2O_3 catalysts probed by positronium. *Atom. Appl. Surf. Sci.* **2013**, *266*, 17–21. [CrossRef]
72. Li, M.; Fang, S.; Hu, Y.H. Self-stabilization of Ni/Al_2O_3 Catalyst with a $NiAl_2O_4$ Isolation Layer in Dry Reforming of Methane. *Catal. Lett.* **2022**, *152*, 2852–2859. [CrossRef]

73. García-Diéguez, M.; Finocchio, E.; Larrubia, M.A.; Alemany, L.J.; Busca, G. Characterization of alumina-supported Pt, Ni and PtNi alloy catalysts for the dry reforming of methane. *J. Catal.* **2010**, *274*, 11–20. [CrossRef]
74. Van Herwijnen, T.; Van Doesburg, H.; De Jong, W.A. Kinetics of the methanation of CO and CO_2 on a nickel catalyst. *J. Catal.* **1973**, *28*, 391–402. [CrossRef]
75. Aksoylu, A.E.; Onsan, Z.L. Hydrogenation of carbon oxides using coprecipitated and impregnated Ni/Al_2O_3 catalysts. *Appl. Catal. A Gen.* **1997**, *164*, 1–11. [CrossRef]
76. Rahmani, S.; Rezaei, M.; Meshkani, F. Preparation of highly active nickel catalysts supported on mesoporous nanocrystalline γ-Al_2O_3 for CO_2 methanation. *J. Ind. Eng. Chem.* **2014**, *20*, 1346–1352. [CrossRef]
77. Beierlein, D.; Häussermann, D.; Pfeifer, M.; Schwarz, T.; Stöwe, K.; Traa, Y.; Klemm, E. Is the CO_2 methanation on highly loaded Ni-Al_2O_3 catalysts really structure sensitive? *Appl. Catal. B Environ.* **2019**, *247*, 200–219. [CrossRef]
78. Lei, H.; Lin, Q.; Huang, Y. Unique catalysis of Ni-Al hydrotalcite derived catalyst in CO_2 methanation: Cooperative effect between Ni nanoparticles and a basic support. *J. Energy Chem.* **2014**, *23*, 587–592.
79. Marocco, P.; Morosanu, E.A.; Giglio, E.; Ferrero, D.; Mebrahtu, C.; Lanzini, A.; Abate, S.; Bensaid, S.; Perathoner, S.; Santarelli, M.; et al. CO_2 methanation over Ni/Al hydrotalcite-derived catalyst: Experimental characterization and kinetic study. *Fuel* **2018**, *225*, 230–242. [CrossRef]
80. Bian, Z.; Chan, Y.M.; Yu, Y.; Kawi, S. Morphology dependence of catalytic properties of Ni/CeO_2 for CO_2 methanation: A kinetic and mechanism study. *Catal. Today* **2020**, *347*, 31–38. [CrossRef]
81. Wang, L.; Zhang, S.; Liu, Y. Reverse water gas shift reaction over Co-precipitated Ni-CeO_2catalysts. *J. Rare Earths* **2008**, *26*, 66–70. [CrossRef]
82. Ye, R.-P.; Li, Q.; Gong, W.; Wang, T.; Razink, J.J.; Lin, L.; Qin, Y.-Y.; Zhou, Z.; Adidharma, H.; Tang, J.; et al. High-performance of nanostructured Ni/CeO_2 catalyst on CO_2 methanation. *Appl. Catal. B Environ.* **2019**, *268*, 118474. [CrossRef]
83. Martin, N.M.; Hemmingsson, F.; Schaefer, A.; Ek, M.; Merte, L.R.; Hejral, U.; Gustafson, J.; Skoglundh, M.; Dippel, A.C.; Gutowski, O.; et al. Structure–function relationship for CO_2 methanation over ceria supported Rh and Ni catalysts under atmospheric pressure conditions. *Catal. Sci. Technol.* **2019**, *9*, 1644. [CrossRef]
84. Li, Z.; Werner, K.; Chen, L.; Jia, A.; Qian, K.; Zhong, J.Q.; You, R.; Wu, L.; Zhang, L.; Pan, H.; et al. Interaction of Hydrogen with Ceria: Hydroxylation, Reduction, and Hydride Formation on the Surface and in the Bulk. *Chem. Eur. J.* **2021**, *27*, 5268–5276. [CrossRef] [PubMed]
85. Deraz, N.M. Effects of heat treatment on physicochemical properties of cerium based nickel system. *J. Anal. Appl. Pyrol.* **2012**, *95*, 56–60. [CrossRef]
86. Padi, S.P.; Shelly, L.; Komarala, E.P.; Schweke, D.; Hayun, S.; Rosen, B.A. Coke-free methane dry reforming over nano-sized NiO-CeO_2 solid solution after exsolution. *Catal. Commun.* **2020**, *138*, 105951. [CrossRef]
87. Wrobel, G.; Sohier, M.P.; D'Huysser, A.; Bonnelle, J.P.; Marcq, J.P. Hydrogenation catalysts based on nickel and rare earth oxides. Part II: XRD, electron microscopy and XPS studies of the cerium-nickel-oxygen-hydrogen system. *Appl. Catal. A Gen.* **1993**, *101*, 73–93. [CrossRef]
88. Ebrahimi, P.; Kumar, A.; Khraisheh, M. A review of recent advances in water-gas shift catalysis for hydrogen production. *Emerg. Mat.* **2020**, *3*, 881–917. [CrossRef]
89. Xie, Y.; Wen, J.; Li, Z.; Chen, J.; Zhang, Q.; Ning, P.; Chen, Y.; Hao, J. Progress in reaction mechanisms and catalyst development of ceria-based catalysts for low-temperature CO_2 methanation. *Green Chem.* **2023**, *25*, 130. [CrossRef]
90. Min, C.; Zanglong, G.; Jian, Z.; Fangli, J.; Wei, C. CO_2 selective hydrogenation to synthetic natural gas (SNG) over four nano-sized Ni/ZrO_2 samples: ZrO_2 crystalline phase & treatment impact. *J. Energy Chem.* **2016**, *25*, 1070–1077.
91. Jia, X.; Zhang, X.; Rui, N.; Hu, X.; Liu, C. Structural effect of Ni/ZrO_2 catalyst on CO_2 methanation with enhanced activity. *Appl. Catal. B Environ.* **2019**, *244*, 159–169. [CrossRef]
92. Tan, J.; Wang, J.; Zhang, Z.; Ma, Z.; Wang, L.; Liu, Y. Highly dispersed and stable Ni nanoparticles confined by MgO on ZrO_2 for CO_2 methanation. *Appl. Surf. Sci.* **2019**, *481*, 1538–1548. [CrossRef]
93. Vargas, E.; Romero-Sáez, M.; Denardin, J.C.; Gracia, F. The ultrasound-assisted synthesis of effective monodisperse nickel nanoparticles: Magnetic characterization and its catalytic activity in CO_2 methanation. *New J. Chem.* **2016**, *40*, 7307–7310. [CrossRef]
94. Ma, L.; Ye, R.; Huang, Y.; Ramirez Reina, T.; Wang, X.; Li, C.; Li, X.; Zhang, L.; Fan, M.; Zhang, R.; et al. Enhanced low-temperature CO_2 methanation performance of Ni/ZrO_2 catalysts via a phase engineering strategy. *Chem. Eng. J.* **2022**, *446*, 137031. [CrossRef]
95. Zhao, K.; Wang, W.; Li, Z. Highly efficient Ni/ZrO_2 catalysts prepared via combustion method for CO_2 methanation. *J. CO_2 Util.* **2016**, *16*, 236–244. [CrossRef]
96. Chandra Bose, A.; Ramamoorthy, R.; Ramasamy, S. Formability of metastable tetragonal solid solution in nanocrystalline NiO–ZrO_2 powders. *Mater. Lett.* **2000**, *44*, 203–207. [CrossRef]
97. Kondo, H.; Sekino, T.; Kusunose, T.; Nakayama, T.; Yamamoto, Y.; Niihara, K. Phase stability and electrical property of NiO-doped yttria-stabilized zirconia. *Mater. Lett.* **2003**, *57*, 1624–1628. [CrossRef]
98. Spennati, E.; Riani, P.; Garbarino, G. A perspective of lanthanide promoted Ni-catalysts for CO_2 hydrogenation to methane: Catalytic activity and open challenges. *Catal. Today* **2023**, *in press*. [CrossRef]
99. Li, Y.; Men, Y.; Liu, S.; Wang, J.; Wang, K.; Tang, Y.; An, W.; Pan, X.; Li, L. Remarkably efficient and stable Ni/Y_2O_3 catalysts for CO_2 methanation: Effect of citric acid addition. *Appl. Catal. B Environ.* **2021**, *293*, 120206. [CrossRef]

100. Ilsemann, J.; Sonström, A.; Gesing, T.M.; Anwander, R.; Bäumer, M. Highly Active Sm_2O_3-Ni Xerogel Catalysts for CO_2 Methanation. *ChemCatChem* **2019**, *11*, 1732–1741. [CrossRef]
101. Tang, G.; Gong, D.; Liu, H.; Wang, L. Highly loaded mesoporous Ni–La_2O_3 catalyst prepared by colloidal solution combustion method for CO_2 methanation. *Catalysts* **2019**, *9*, 442. [CrossRef]
102. Ebrahimi, P.; Kumar, A.; Khraisheh, M. Combustion synthesis of lanthanum oxide supported Cu, Ni, and CuNi nanoparticles for CO_2 conversion reaction. *Int. J. Hydrogen Energy* **2022**, *in press*. [CrossRef]
103. Valsamakis, I.; Garbarino, G. Lanthanum-based catalysts for (bio)ethanol conversion: Effect of preparation method on catalytic performance—hard templating versus hydrolysis. *J. Chem. Technol. Biotechnol.* **2021**, *96*, 1116–1124. [CrossRef]
104. Dai, Y.; Xu, M.; Wang, Q.; Huang, R.; Jin, Y.; Bian, B.; Tumurbaatar, C.; Ishtsog, B.; Bold, T.; Yang, Y. Enhanced activity and stability of Ni/$La_2O_2CO_3$ catalyst for CO_2 methanation by metal-carbonate interaction. *Appl. Catal. B Environ.* **2020**, *277*, 119271. [CrossRef]
105. Unwiset, P.; Chanapattharapol, K.C.; Kidkhunthod, P.; Poo-arporn, Y.; Ohtani, B. Catalytic activities of titania-supported nickel for carbon-dioxide methanation. *Chem. Energy Sci.* **2020**, *228*, 115955. [CrossRef]
106. Hanaor, D.A.H.; Sorrel, C.C. Review of the anatase to rutile phase transformation. *J. Mater. Sci.* **2011**, *46*, 855–874. [CrossRef]
107. Santamaria, L.; Lopez, G.; Arregi, A.; Amutio, M.; Artetxe, M.; Bilbao, J.; Olazar, M. Stability of different Ni supported catalysts in the in-line steam reforming of biomass fast pyrolysis volatiles. *Appl. Catal. B Environ.* **2019**, *242*, 109–120. [CrossRef]
108. Messou, D.; Bernardin, V.; Meunier, F.; Borges Ordoño, M.; Urakawa, A.; Machado, B.F.; Collière, V.; Philippe, R.; Serp, P.; Le Berre, C. Origin of the synergistic effect between TiO_2 crystalline phases in the Ni/TiO_2-catalyzed CO_2 methanation reaction. *J. Catal.* **2021**, *398*, 14–28. [CrossRef]
109. Nakayama, T.; Ichikuni, N.; Sato, S.; Nozaki, F. Ni/Mgo catalyst prepared using citric acid for hydrogenation of carbon dioxide. *Appl. Catal. A Gen.* **1997**, *158*, 185–199. [CrossRef]
110. Loder, M.A.; Siebenhofer, S.L. The reaction kinetics of CO_2 methanation on a bifunctional Ni/MgO catalyst. *J. Ind. Eng. Chem.* **2020**, *85*, 196–207. [CrossRef]
111. Aneggi, E.; Boaro, M.; Colussi, S.; de Leitenburg, C.; Trovarelli, A. Chapter 289—Ceria-Based Materials in Catalysis: Historical Perspective and Future Trends. In *Handbook on the Physics and Chemistry of Rare Earths*; Elsevier: Amsterdam, The Netherlands, 2016; Volume 50, pp. 209–242.
112. Busca, G. Silica-alumina catalytic materials: A critical review. *Catal. Today* **2020**, *357*, 621–629. [CrossRef]
113. Liang, C.; Ye, Z.; Dong, D.; Zhang, S.; Liu, Q.; Chen, G.; Li, C.; Wang, Y.; Hu, X. Methanation of CO_2: Impacts of modifying nickel catalysts with variable valence additives on reaction mechanism. *Fuel* **2019**, *254*, 115654. [CrossRef]
114. Cai, M.; Wen, J.; Chu, W.; Cheng, X.; Li, Z. Methanation of carbon dioxide on Ni/ZrO_2-Al_2O_3 catalysts: Effects of ZrO_2 promoter and preparation method of novel ZrO_2-Al_2O_3 carrier. *J. Nat. Gas Chem.* **2011**, *20*, 318–324. [CrossRef]
115. Ahmad, W.; Younis, M.N.; Shawabkeh, R.; Ahmed, S. Synthesis of lanthanide series (La, Ce, Pr, Eu & Gd) promoted Ni/γ-Al_2O_3 catalysts for methanation of CO_2 at low temperature under atmospheric pressure. *Catal. Commun.* **2017**, *100*, 121–126. [CrossRef]
116. Guilera, J.; del Valle, J.; Alarcon, A.; Díaz, J.A.; Andreu, T. Metal-oxide promoted Ni/Al_2O_3 as CO_2 methanation micro-size catalysts. *J. CO_2 Util.* **2019**, *30*, 11–17. [CrossRef]
117. Kim, M.J.; Youn, J.R.; Kim, H.J.; Seo, M.W.; Lee, D.; Go, K.S.; Lee, K.B.; Jeon, S.G. Effect of surface properties controlled by Ce addition on CO_2 methanation over Ni/Ce/Al_2O_3 catalyst. *Int. J. Hydrogen Energy* **2020**, *45*, 24595–24603. [CrossRef]
118. Riani, P.; Valsamakis, I.; Cavattoni, T.; Sanchez Escribano, V.; Busca, G.; Garbarino, G. Ni/SiO_2-Al_2O_3 catalysts for CO_2 methanation: Effect of La_2O_3 addition. *Appl. Catal. B Envir.* **2021**, *284*, 119697. [CrossRef]
119. Gandara-Loe, J.; Portillo, E.; Odriozola, J.A.; Reina, T.R.; Pastor-Pérez, L. K-Promoted Ni-Based Catalysts for Gas-Phase CO_2 Conversion: Catalysts Design and Process Modelling Validation. *Front. Chem.* **2021**, *9*, 785571. [CrossRef] [PubMed]
120. Liang, C.; Hu, X.; Wei, T.; Jia, P.; Zhang, Z.; Dong, D.; Zhang, S.; Liu, Q.; Hu, G. Methanation of CO_2 over Ni/Al_2O_3 modified with alkaline earth metals: Impacts of oxygen vacancies on catalytic activity. *Int. J. Hydrogen Energy* **2019**, *44*, 8197–8213. [CrossRef]
121. Garbarino, G.; Pugliese, F.; Cavattoni, T.; Busca, G.; Costamagna, P. A Study on CO_2 Methanation and Steam Methane Reforming over Commercial Ni/Calcium Aluminate Catalysts. *Energies* **2020**, *13*, 2792. [CrossRef]
122. Garbarino, G.; Kowalik, P.; Riani, P.; Antoniak-Jurak, K.; Pieta, P.; Lewalska-Graczyk, A.; Lisowski, W.; Nowakowski, R.; Busca, G.; Pieta, I.S. Improvement of Ni/Al_2O_3 catalysts for low-temperature CO_2 methanation by vanadium and calcium oxide addition. *Ind. Eng. Chem. Res.* **2021**, *60*, 655–664. [CrossRef]
123. Liu, J.; Bing, W.; Xue, X.; Wang, F.; Wang, B.; He, S.; Zhang, Y.; Wei, M. Alkaline-assisted Ni nanocatalysts with largely enhanced low-temperature activity toward CO_2 methanation. *Catal. Sci. Technol.* **2016**, *6*, 3976. [CrossRef]
124. Fasolini, A.; Spennati, E.; Atakoohi, S.E.; Percivale, M.; Busca, G.; Basile, F.; Garbarino, G. A study of CO_2 hydrogenation over Ni-MgAlOx catalysts derived from hydrotalcite precursors. *Catal. Today* **2023**, *423*, 114271. [CrossRef]
125. Zhao, K.; Li, Z.; Bian, L. CO_2 methanation and co-methanation of CO and CO_2 over Mn-promoted Ni/Al_2O_3 catalysts. *Front. Chem. Sci. Eng.* **2016**, *10*, 273–280. [CrossRef]
126. Vrijburg, W.L.; Garbarino, G.; Chen, W.; Parastaev, A.; Longo, A.; Pidko, E.A.; Hensen, E.J.M. Ni-Mn catalysts on silica-modified alumina for CO_2 methanation. *J. Catal.* **2020**, *382*, 358–371. [CrossRef]
127. Wu, Y.; Lin, J.; Xu, Y.; Ma, G.; Wang, J.; Ding, M. Transition Metals Modified Ni−M (M = Fe, Co, Cr and Mn) Catalysts Supported on $Al_2O3-ZrO_2$ for Low-Temperature CO_2 Methanation. *ChemCatChem* **2020**, *12*, 3553–3559. [CrossRef]

128. Pan, Q.; Peng, J.; Sun, T.; Wang, S.; Wang, S. Insight into the reaction route of CO_2 methanation: Promotion effect of medium basic sites. *Catal. Commun.* **2014**, *45*, 74–78. [CrossRef]
129. Ullah, N.; Tang, R.; Li, Z. Nanostructured Ceria-zirconia Supported Ni Catalysts for High Performance CO_2 Methanation: Phase and morphology effect on activity. *J. Taiwan Inst. Chem. Eng.* **2022**, *134*, 104317. [CrossRef]
130. Zhang, Z.; Yu, Z.; Feng, K.; Yan, B. Eu^{3+} doping-promoted Ni-CeO_2 interaction for efficient low-temperature CO_2 methanation. *Appl. Catal. B Environ.* **2022**, *317*, 121800. [CrossRef]
131. Liu, F.; Park, Y.S.; Diercks, D.; Kazempoor, P.; Duan, C. Enhanced CO_2 methanation activity of $Sm_{0.25}Ce_{0.75}O_{2-\delta}$-Ni by modulating the chelating agents-to-metal cation ratio and tuning metal-support interaction. *ACS Appl. Mater. Interfaces* **2022**, *14*, 13295–13304. [CrossRef]
132. Sun, C.; Beaunier, P.; La Parola, V.; Liotta, L.F.; Da Costa, P. Ni/CeO_2 nanoparticles promoted by yttrium doping as catalysts for CO_2 methanation. *ACS Appl. Nano Mater.* **2020**, *3*, 12355–12368. [CrossRef]
133. Siakavelas, G.I.; Charisiou, N.D.; Alkhoori, A.; Alkhoori, S.; Sebastian, V.; Hinder, S.J.; Baker, M.A.; Yentekakis, I.V.; Polychronopoulou, K.; Goula, M.A. Highly selective and stable Ni/La-M (M=Sm, Pr, and Mg)-CeO_2 catalysts for CO_2 methanation. *J. CO_2 Util.* **2021**, *51*, 101618. [CrossRef]
134. Liu, K.; Xu, X.; Xu, J.; Fang, X.; Liu, L.; Wang, X. The distributions of alkaline earth metal oxides and their promotional effects on Ni/CeO_2 for CO_2 methanation. *J. CO_2 Util.* **2020**, *38*, 113–124. [CrossRef]
135. Mihet, M.; Lazar, M.D. Methanation of CO_2 on Ni/γ-Al_2O_3: Influence of Pt, Pd or Rh promotion. *Catal. Today* **2018**, *306*, 294–299. [CrossRef]
136. Pan, Y.; Han, X.; Chang, X.; Zhang, H.; Zi, X.; Hao, Z.; Chen, J.; Lin, Z.; Li, M.; Ma, X. Enhanced Low-Temperature CO_2 Methanation over Bimetallic Ni–Ru Catalysts. *Ind. Eng. Chem. Res.* **2023**, *62*, 4344–4355. [CrossRef]
137. Summa, P.; Świrk Da Costa, K.; Wang, Y.; Samojeden, B.; Rønning, M.; Hu, C.; Motak, M.; Da Costa, P. Effect of cobalt promotion on hydrotalcite-derived nickel catalyst for CO_2 methanation. *Appl. Mater. Today* **2021**, *25*, 101211. [CrossRef]
138. Huynh, H.L.; Zhu, J.; Zhang, Y.; Shen, Y.; Mekonnen Tucho, W.; Ding, Y.; Yu, Z. Promoting effect of Fe on supported Ni catalysts in CO_2 methanation by in situ DRIFTS and DFT study. *J. Catal.* **2020**, *392*, 266–277. [CrossRef]
139. Xu, L.; Cui, Y.; Chen, M.; Wen, X.; Lv, C.; Wu, X.; Wu, C.; Miao, Z.; Hu, X. Screening Transition Metals (Mn, Fe, Co, and Cu) Promoted Ni-Based CO_2 Methanation Bimetal Catalysts with Advanced Low Temperature Activities. *Ind. Eng. Chem. Res.* **2021**, *60*, 8056–8072. [CrossRef]
140. Heine, C.; Lechner, B.A.J.; Bluhm, H.; Salmeron, M. Recycling of CO_2: Probing the Chemical State of The Ni(111) Surface During the Methanation Reaction with Ambient-pressure X-ray Photoelectron Spectroscopy. *J. Am. Chem. Soc.* **2016**, *138*, 13246–13252. [CrossRef]
141. Huang, M.-X.; Liu, F.; He, C.-C.; Yang, S.-Q.; Chen, W.Y.; Ouyang, L.; Zhao, Y.-J. Interface promoted CO_2 methanation: A theoretical study of Ni/La_2O_3. *Chem. Phys. Lett.* **2021**, *768*, 138396. [CrossRef]
142. Sanchez-Escribano, V.; Larrubia Vargas, M.A.; Finocchio, E.; Busca, G. On the mechanisms and the selectivity determining steps in syngas conversion over supported metal catalysts: An IR study. *Appl. Catal. A Gen.* **2007**, *316*, 68–74. [CrossRef]
143. Solis-Garcia, A.; Louvier-Hernandez, J.F.; Almendarez-Camarillo, A.; Fierro-Gonzalez, J.C. Participation of surface bicarbonate, formate and methoxy species in the carbon dioxide methanation catalyzed by ZrO_2-supported Ni. *Appl. Catal. B Environ.* **2017**, *218*, 611–620. [CrossRef]
144. Breysse, M.; Afanasiev, P.; Geantet, C.; Vrinat, M. Overview of support effects in hydrotreating catalysts. *Catal. Today* **2003**, *86*, 5–16. [CrossRef]